

Computing Sound and Accurate Upper and Lower Bounds on Hamilton-Jacobi Reachability Value Functions

Ihab Tabbara

i.k.tabbara@wustl.edu

Washington University in St. Louis
St. Louis, MO, USA

Eliya Badr

egb11@mail.aub.edu

American University of Beirut
Beirut, Lebanon

Hussein Sibai

sibai@wustl.edu

Washington University in St. Louis
St. Louis, MO, USA

Abstract

Hamilton-Jacobi (HJ) reachability analysis is a fundamental tool for safety verification and control synthesis for nonlinear-control systems. Classical HJ reachability analysis methods discretize the continuous state space and solve the HJ partial differential equation over a grid, but these approaches do not account for discretization errors and can under-approximate backward reachable sets, which represent unsafe sets of states. We present a framework for computing sound upper and lower bounds on the HJ value functions via value iteration over grids. Additionally, we develop a refinement algorithm that splits cells that were not possible to classify as safe or unsafe given the computed bounds. This algorithm enables computing accurate over-approximations of backward reachable sets even when starting from coarse grids. Finally, we validate the effectiveness of our method in two case studies.

Keywords

Hamilton-Jacobi reachability analysis, Formal verification, Reinforcement learning, Safe control

1 Introduction

Ensuring safety of control systems is crucial, especially those deployed in safety-critical settings, such as autonomous driving [5], surgical robotics [7], and aerospace [8]. Among the various approaches to address this challenge, Hamilton-Jacobi (HJ) reachability analysis [13, 14] has emerged as a fundamental technique for safety verification and control synthesis. Given a user-defined failure set of states \mathcal{F} that the system must avoid reaching, HJ reachability analysis computes the corresponding backward reachable set (BRS), which is the set of all states from which reaching the failure set cannot be prevented despite the best control effort. The BRS is represented as the sub-zero level set of a value function.

Existing HJ reachability analysis methods [4, 9, 14] solve the HJ partial differential equation (PDE) numerically on a grid that discretizes the continuous state space. By solving the HJ PDE over a grid without explicitly accounting for discretization errors, these methods can result in sets which under-approximate the true BRS, leading to unsafe states, i.e., states in the true BRS, being incorrectly classified as safe, as recently demonstrated in [12] and as we illustrate in Section 9. In this paper, we develop a framework for computing sound lower and upper bounds on the HJ reachability value function that can be used to generate sound and accurate over-approximations of the BRS.

The recent work of Li et al. [11] introduced a discounted reach-avoid value function, proved that it is Lipschitz continuous, and showed that its sub-zero and super-zero level sets are the same as those of the non-discounted reach-avoid value function. Inspired by

this work, we formulate a discounted avoid-only reachability value function whose sub-zero level set is the true BRS. We show that its Bellman operator is a contraction mapping. Then, we partition the state space into a finite grid and compute two value functions over the grid: an upper bound \bar{V}_γ and a lower bound \underline{V}_γ . These functions provably bound the true value function V_γ over the continuous state space from both sides, which allows sound over-approximation of the BRS.

We compute the bounding functions using value iteration. Since convergence of value iteration generally requires infinitely many iterations, it is usually terminated once the successive-iterate gap falls below a user-specified tolerance (e.g., $\|V^{(k+1)} - V^{(k)}\|_\infty \leq \varsigma$). Following this approach and using non-converged iterates can affect the soundness of our method. For example, the current lower-bound iterate $\underline{V}_\gamma^{(k)}$ may still overestimate the fixed-point lower bound, potentially leading to miss-classifying unsafe states as safe. We account for such early-termination errors when computing the lower bound to maintain its soundness. For the upper bound, we prove that any iterate $\bar{V}_\gamma^{(k)}$ is guaranteed to upper bound the true value function when initialized appropriately.

Finally, we provide an algorithm, which automatically and locally refines the grid by splitting cells that were not yet classified as safe or unsafe. By iteratively refining these cells, our algorithm obtains more accurate over-approximations of the BRS. We validate our theory using two case studies.

Our main contributions are summarized below:

- we present an algorithm for computing sound overapproximations of BRSs of discrete-time nonlinear control systems while accounting for discretization errors resulting from gridding the state space and approximation errors resulting from the early termination of value iteration, providing sound upper and lower bounds on the true HJ reachability value functions;
- we develop a refinement algorithm that splits the cells in the grid which could not be classified as safe or unsafe to obtain more accurate over-approximations of the BRS.

2 Related works

Existing HJ reachability analysis methods [4, 10, 14] discretize the state space into grid cells, and use level set methods to solve a time-dependent HJ PDE by evaluating the solution only at the centers of those cells. These approaches offer little guidance for selecting appropriate grid resolutions and are not guaranteed to result in sound over-approximations of the BRSs. Our method instead computes sound upper and lower bounds on the value function that account for discretization errors. Furthermore, we introduce a refinement algorithm that eliminates the need for pre-specifying sufficiently

fine grid resolutions by automatically refining cells that were not possible to classify as safe or unsafe given the computed bounds in an attempt to get tighter bounds that allow their classification.

A close work to ours is the recent work by Liu and Mallada [12], introducing Recurrent Control Barrier Functions (RCBFs) which relax the strict invariance requirement of traditional CBFs [2, 3] by requiring only finite-time (τ) recurrence to the safe set. They provide an algorithm that computes sound under-approximation of the safe set, and thus a sound over-approximation of the unsafe one as well. They also develop a highly parallelizable data-driven nonparametric method to compute safe sets and show that their method is more efficient than existing HJ toolboxes [9] when used for the computation of safe sets.

Our approach to constructing upper and lower bounds for the HJ value function is inspired by the work of Alaoui et al. [1], who propose a symbolic control framework for Q-learning in continuous state-action spaces. They construct discrete abstractions and introduce a Q-learning algorithm that produces two Q-tables providing upper and lower bounds on the continuous Q-function. Our work differs in several aspects. First, their Q-learning value functions differ in their forms from HJ reachability value functions. Second, their problem setting of reinforcement learning does not require different approximation accuracies of the Q-function, while in HJ reachability analysis, areas in the state space near the boundary of the BRS require more accurate approximations of the value function. More specifically, HJ reachability analysis only needs to determine whether states belong to the super-zero or sub-zero level sets of the true HJ reachability value function to characterize the backward reachable set, which motivates our development of an adaptive refinement algorithm to split only unclassified boundary cells. Third, we address early termination errors in value iteration to maintain the soundness of our safety guarantees, while their framework does not address this issue.

Li et al. [11] recently proposed training neural networks to approximate discounted reach-avoid value functions using deep reinforcement learning, then certify whether neighborhoods around individual query states belong to the reach-avoid sets. Their certification can be performed online for queried states or offline by enumerating a finite sets of sample states whose neighborhoods cover regions of interest. In contrast, our method does not rely on machine learning and instead performs offline computation of provable upper and lower bounds on the HJ value function through value iteration.

3 Preliminaries

We consider systems with deterministic discrete-time dynamics of the form

$$x_{t+1} = f(x_t, u_t), \quad (1)$$

where $x_t \in \mathcal{X} \subseteq \mathbb{R}^n$ denotes the system state at time t , $u_t \in \mathcal{U} \subseteq \mathbb{R}^m$ denotes the control input at time t , \mathcal{U} is a compact set, and $f : \mathcal{X} \times \mathcal{U} \rightarrow \mathbb{R}^n$ is a nonlinear globally Lipschitz continuous function in the first argument with Lipschitz constant L_f . A policy is a mapping $\pi : \mathbb{R}^n \rightarrow \mathcal{U}$. We denote the trajectory with initial state $x \in \mathcal{X}$ and following π by $\xi_x^\pi := \{x_t\}_{t \geq 0}$.

We encode a user-defined failure set $\mathcal{F} \subseteq \mathcal{X}$ as the *sub-zero level set* of a Lipschitz continuous function $l : \mathbb{R}^n \rightarrow \mathbb{R}$ with a known Lipschitz constant $L_l > 0$, i.e., $\mathcal{F} := \{x \in \mathcal{X} \mid l(x) \leq 0\}$.

Discounted avoid measure and safety value. Fix a discount factor $\gamma \in (0, 1)$. For a finite horizon $t \in \mathbb{N}$, define the *discounted avoid measure*

$$g_\gamma(\xi_x^\pi, t) := \min_{\tau=0, \dots, t} \gamma^\tau l(x_\tau), \quad (2)$$

whose, more general, reach-avoid version was introduced in [11]. The corresponding (*avoid*) *reachability value function* is defined as follows:

$$V_\gamma(x) := \max_{\pi} \sup_{t \geq 0} g_\gamma(\xi_x^\pi, t) = \max_{\pi} \sup_{t \geq 0} \min_{\tau \leq t} \gamma^\tau l(x_\tau). \quad (3)$$

Intuitively, g_γ evaluates the *worst discounted safety margin* encountered along a trajectory up to time t , while $V_\gamma(x)$ represents the supremum of this worst-case margin obtained by any feasible policy unrolled for any horizon t starting from state x . Consequently, the super-zero level set of V_γ characterizes the *safe set* of states: $\{x \mid V_\gamma(x) > 0\}$, which represents the states starting from which and following the policy that maximizes V_γ avoids \mathcal{F} at all times. On the other hand, its complement, $\mathcal{L}_\gamma := \{x \in \mathcal{X} \mid V_\gamma(x) \leq 0\}$ is the *unsafe set*.

As shown in [11], the super-zero level set for a discounted reach-avoid value function, defined in a similar manner to V_γ in (3) but with including a *reach* constraint, coincides with the true reach-avoid set for any $\gamma \in (0, 1)$, without requiring annealing γ to 1, which was needed in previous formulations of the reach-avoid value function. In this work, we adapt the framework of [11] to the avoid-only setting by defining an analogous discounted avoid measure $g_\gamma(\xi_x^\pi, t)$ in (2). By a similar argument to the one in [11], for any γ , \mathcal{L}_γ coincides with the true BRS, which is the set of states starting from which there is no policy that can guarantee avoiding \mathcal{F} . Thus, we drop the γ subscript from \mathcal{L}_γ and call it \mathcal{L} for the rest of the paper.

We first derive the corresponding Bellman operator for the value function defined in (3) and establish its contraction property in Theorem 1.

Dynamic programming and the Bellman equation. Starting from (2)–(3), we proceed with the recursion: consider any trajectory $\{x_\tau\}_{\tau \geq 0}$, then for any $t \geq 0$,

$$\min_{\tau \leq t} \gamma^\tau l(x_\tau) = \min \{l(x_0), \gamma \min_{\tau \leq t-1} \gamma^\tau l(x_{\tau+1})\}.$$

Taking $\sup_{t \geq 0}$ on both sides gives

$$\sup_{t \geq 0} \min_{\tau \leq t} \gamma^\tau l(x_\tau) = \min \{l(x_0), \gamma \sup_{t \geq 0} \min_{\tau \leq t} \gamma^\tau l(x_{\tau+1})\}.$$

Applying \max_π to both sides and knowing that maximization over policies is equivalent to maximization over the immediate control action followed by a maximization over all policies from the subsequent state, we get:

$$V_\gamma(x) = \min \left\{ l(x), \max_{u \in \mathcal{U}} \gamma V_\gamma(f(x, u)) \right\}, \quad (4)$$

which can be seen as the avoid-only analogue of the discounted reach-avoid Bellman equation in [11]. Consequently, we define the

Bellman operator \mathcal{T}_Y as follows

$$(\mathcal{T}_Y V_Y)(x) := \min \left\{ l(x), \max_{u \in \mathcal{U}} \gamma V_Y(f(x, u)) \right\}. \quad (5)$$

A key property of the Bellman operator \mathcal{T}_Y is that it is a contraction mapping, which guarantees the existence and uniqueness of the value function V_Y and ensures that the value iteration algorithm converges to the fixed point. We establish this property in the following theorem.

Theorem 1 (Contraction and uniqueness). For any $\gamma \in (0, 1)$ and any bounded functions $V_{Y,1} : \mathcal{X} \rightarrow \mathbb{R}$, $V_{Y,2} : \mathcal{X} \rightarrow \mathbb{R}$, we have

$$\|\mathcal{T}_Y V_{Y,1} - \mathcal{T}_Y V_{Y,2}\|_\infty \leq \gamma \|V_{Y,1} - V_{Y,2}\|_\infty. \quad (6)$$

Hence \mathcal{T}_Y is a γ -contraction in $(\mathcal{B}(\mathbb{R}^n), \|\cdot\|_\infty)$, the space of bounded real-valued functions on \mathbb{R}^n , with the supremum norm as its norm. It admits the unique fixed point V_Y .

PROOF. Fix any state $x \in \mathcal{X}$. By the non-expansiveness of the min operator, we have

$$\begin{aligned} |(\mathcal{T}_Y V_{Y,1})(x) - (\mathcal{T}_Y V_{Y,2})(x)| &\leq \left| \max_{u \in \mathcal{U}} \gamma V_{Y,1}(f(x, u)) \right. \\ &\quad \left. - \max_{u \in \mathcal{U}} \gamma V_{Y,2}(f(x, u)) \right|. \end{aligned}$$

Knowing that the max operator is non-expansive and factoring out γ yields

$$\begin{aligned} \left| \max_{u \in \mathcal{U}} \gamma V_{Y,1}(f(x, u)) - \max_{u \in \mathcal{U}} \gamma V_{Y,2}(f(x, u)) \right| &\leq \\ \gamma \max_{u \in \mathcal{U}} |V_{Y,1}(f(x, u)) - V_{Y,2}(f(x, u))| &\leq \gamma \|V_{Y,1} - V_{Y,2}\|_\infty. \end{aligned}$$

Taking the supremum over $x \in \mathcal{X}$ results in (6). \square

The results established thus far characterize the reachability value function V_Y over the continuous state space $\mathcal{X} \subseteq \mathbb{R}^n$. However, computing V_Y exactly for nonlinear systems is generally intractable. Existing approaches approximate it by considering only the centers of the cells of a grid over the state space during its computation. Instead, we bound its values at all states by computing two value functions over the grid.

4 Discrete abstractions

To bound V_Y , we build a *discrete abstraction* \mathcal{A} of system (1) [15]. The abstraction \mathcal{A} has a finite set of states S representing the cells in a grid \mathcal{G} over \mathcal{X} , a finite set of controls A , and a non-deterministic transition relation Δ that maps state-action pairs to subsets of S . The set of control actions A is a finite subset of \mathcal{U} . One can, for example, construct A as the set of centers of the cells of a grid over \mathcal{U} . To compute the transition relation Δ , we compute the reachable sets of system (1) starting from each cell as the set of initial states and following each of the discrete control actions.

We denote the one time-step reachable set starting from the cell represented by $s \in S$ and following control action $a \in A$ by $R(s, a) := \bigcup_{x \in [[s]]} \{f(x, a)\}$, where $[[s]]$ represent the set of states in \mathcal{X} that belong to the cell in \mathcal{G} represented by s . We abuse notation and call that cell s as well.

One can compute an over-approximation of $R(s, a)$ by simulating system (1) forward starting from $x_c(s)$, the center of the cell s , following a and then constructing a ball of radius $L_f \max_i \eta_i(s)$, where $\eta \in (\mathbb{R}^+)^n$ represent the radii in every dimension of the cell

s , i.e., half of the side length in every dimension. More formally, $R(s, a) \subseteq B_{\max_{i \in [n]} \eta_i(s)}(f(x_c(s), a))$, where $B_r(x)$ is the ball of radius r , i.e., a hypercube of sides equal to $2r$, centered at $x \in \mathcal{X}$. This follows from L_f being the global Lipschitz constant of f .

Given an over-approximation of the reachable set, which we also denote by R , we can construct the non-deterministic transition relation $\Delta : S \times A \rightarrow 2^S$ as follows: $\forall s, s' \in S, \forall a \in A,$

$$s' \in \Delta(s, a) \text{ iff } [[s']] \cap R(s, a) \neq \emptyset. \quad (7)$$

We define Δ similarly when using any action $u \in \mathcal{U}$ that does not necessarily belongs to A .

5 Value function bounds

To bound V_Y , we first need to bound the failure function l . We construct upper and lower bounds on the values l can have at the states in each cell of the grid \mathcal{G} . Since l is L_l -Lipschitz, then $\forall s \in S, \forall x \in [[s]], |l(x) - l(x_c(s))| \leq L_l \|x - x_c(s)\|_\infty \leq L_l \max_{i \in [n]} \eta_i(s)$, where $\eta \in (\mathbb{R}^{\geq 0})^n$ represents the radii of the cell s in the infinite norm sense. Thus, for all $s \in S$, we define $\underline{l}(s) := l(x_c(s)) - L_l \max_{i \in [n]} \eta_i(s)$ and $\bar{l}(s) := l(x_c(s)) + L_l \max_{i \in [n]} \eta_i(s)$ so that $\forall x \in [[s]], \underline{l}(s) \leq l(x) \leq \bar{l}(s)$.

Using these cell-wise bounds on l , we define functions over S to upper and lower bound V_Y over the continuous states in \mathcal{X} as follows:

$$\bar{V}_Y(s) := \min \left\{ \bar{l}(s), \max_{u \in \mathcal{U}} \max_{s' \in \Delta(s, u)} \gamma \bar{V}_Y(s') \right\}, \quad (8)$$

$$\underline{V}_Y(s) := \min \left\{ \underline{l}(s), \max_{u \in \mathcal{U}} \min_{s' \in \Delta(s, u)} \gamma \underline{V}_Y(s') \right\}. \quad (9)$$

It follows that $\forall s \in S, \forall x \in [[s]], \underline{V}_Y(s) \leq V_Y(x) \leq \bar{V}_Y(s)$. Thus, if $\underline{V}_Y(s) > 0$, then $[[s]] \cap \mathcal{L} = \emptyset$, i.e., every state x in the cell s is safe, and if $\bar{V}_Y(s) \leq 0$, then $[[s]] \subseteq \mathcal{L}$, i.e., every state x in the cell s is unsafe. This result follows from the assumption that $\Delta(s, u)$ over-approximates the set of states in S reached by following u starting from s , i.e., the cells in $\Delta(s, u)$ contain all the continuous states in \mathcal{X} that can be reached by system (1) by following the control u starting from a state in $[[s]]$.

Note that the maximums in (8) and (9) are taken over \mathcal{U} , but computing such a maximums, which include characterizing $\Delta(s, u)$ for every $u \in \mathcal{U}$ might not be feasible. If the maximum were taken over the subset A of \mathcal{U} instead, then the resulting functions \bar{V}_Y^A and \underline{V}_Y^A would be smaller, entry-wise, than \bar{V}_Y and \underline{V}_Y as defined in (8) and (9), respectively. In that case, the resulting lower bound can be used to classify safe states but the upper bound might not be reliable for classifying unsafe states.

For the remaining of this paper, value functions with superscript A (i.e., \underline{V}_Y^A and \bar{V}_Y^A) denote the resulting value functions when the maximization in (8) and (9) is taken over A , while those without (i.e., \underline{V}_Y and \bar{V}_Y) denote maximization over \mathcal{U} ; we discuss the implications of this distinction when presenting the guarantees of Algorithm 1 in Theorem 2.

One can compute \underline{V}_Y and \bar{V}_Y using value iteration by iteratively applying the Bellman operator until convergence. Value iteration converges to the fixed point as the number of iterations approaches infinity. However, in practice, we must terminate the algorithm

after a finite number of iterations, which introduces an approximation error. One should account for such errors to provide sound approximations of the continuous V_γ . Specifically, upon termination of the value iteration algorithm in finite number of iterations, the resulting function may overestimate the true value function V_γ , which can potentially lead to classifying unsafe states as safe.

6 Early stopping of value iteration

In this section, we discuss how to account for the errors resulting from early termination of the value iteration algorithm when computing \underline{V}_γ and \bar{V}_γ .

Let $\underline{V}_\gamma^{(k)}$ and $\bar{V}_\gamma^{(k)}$ denote the functions computed by the value iteration algorithm at iteration k when computing \underline{V}_γ and \bar{V}_γ that are initialized as follows: $\forall s \in S, \underline{V}_\gamma^{(0)}(s) = \underline{l}(s)$ and $\bar{V}_\gamma^{(0)}(s) = \bar{l}(s)$.

Lemma 1. For any iteration $k \geq 1$ of the value iteration algorithm computing \underline{V}_γ , define $\underline{\delta}_k := \min_{s \in S} (\underline{V}_\gamma^{(k)}(s) - \underline{V}_\gamma^{(k-1)}(s))$. Then, $\forall k \geq 0, \forall s \in S$,

$$\underline{V}_\gamma^{(k)}(s) + \gamma \underline{\delta}_k \leq \underline{V}_\gamma^{(k+1)}(s) \leq \underline{V}_\gamma^{(k)}(s).$$

PROOF. We first prove that $\forall k \in \mathbb{N}, \forall s \in S, \underline{V}_\gamma^{(k+1)}(s) \leq \underline{V}_\gamma^{(k)}(s)$ by induction. Base case: by definition,

$$\underline{V}_\gamma^{(1)}(s) = \min \left\{ \underline{l}(s), \max_{u \in \mathcal{U}} \min_{s' \in \Delta(s, u)} \gamma \underline{V}_\gamma^{(0)}(s') \right\}.$$

Thus, $\forall s \in S, \underline{V}_\gamma^{(1)}(s) \leq \underline{l}(s)$, and the latter is equal to $\underline{V}_\gamma^{(0)}(s)$, proving the base case. Next, fix a $k \geq 0$ and assume now for the sake of induction that $\forall s \in S, \underline{V}_\gamma^{(k+1)}(s) \leq \underline{V}_\gamma^{(k)}(s)$. We will prove that $\forall s \in S, \underline{V}_\gamma^{(k+2)}(s) \leq \underline{V}_\gamma^{(k+1)}(s)$. Again, by definition, $\forall s \in S$,

$$\underline{V}_\gamma^{(k+2)}(s) = \min \left\{ \underline{l}(s), \max_{u \in \mathcal{U}} \min_{s' \in \Delta(s, u)} \gamma \underline{V}_\gamma^{(k+1)}(s') \right\}.$$

However, $\forall s' \in S, \underline{V}_\gamma^{(k+1)}(s') \leq \underline{V}_\gamma^{(k)}(s')$, by the induction hypothesis. Thus, $\forall s \in S$,

$$\underline{V}_\gamma^{(k+2)}(s) \leq \min \left\{ \underline{l}(s), \max_{u \in \mathcal{U}} \min_{s' \in \Delta(s, u)} \gamma \underline{V}_\gamma^{(k)}(s') \right\}.$$

But the right-hand-side of the inequality above is equal to $\underline{V}_\gamma^{(k+1)}(s)$, by definition. Consequently, $\forall s \in S, \underline{V}_\gamma^{(k+2)}(s) \leq \underline{V}_\gamma^{(k+1)}(s)$. It follows that $\forall k \in \mathbb{N}, \underline{\delta}_k \leq 0$.

Now, fix any $s \in S$, any $u \in \mathcal{U}$, and any successor $s' \in \Delta(s, u)$, we have by the definition of $\underline{\delta}_k$ that

$$\underline{V}_\gamma^{(k)}(s') \geq \underline{V}_\gamma^{(k-1)}(s') + \underline{\delta}_k.$$

Multiplying by γ on both sides results in $\gamma \underline{V}_\gamma^{(k)}(s') \geq \gamma \underline{V}_\gamma^{(k-1)}(s') + \gamma \underline{\delta}_k$. Then, $\max_{u \in \mathcal{U}} \min_{s' \in \Delta(s, u)} \gamma \underline{V}_\gamma^{(k)}(s') \geq \max_{u \in \mathcal{U}} \min_{s' \in \Delta(s, u)} \gamma \underline{V}_\gamma^{(k-1)}(s') + \gamma \underline{\delta}_k$.

$\gamma \underline{V}_\gamma^{(k-1)}(s') + \gamma \underline{\delta}_k$. Finally, taking the minimum with $\underline{l}(s)$ gives

$$\begin{aligned} \underline{V}_\gamma^{(k+1)}(s) &= \min \left\{ \underline{l}(s), \max_{u \in \mathcal{U}} \min_{s' \in \Delta(s, u)} \gamma \underline{V}_\gamma^{(k)}(s') \right\} \\ &\geq \min \left\{ \underline{l}(s), \max_{u \in \mathcal{U}} \min_{s' \in \Delta(s, u)} \gamma \underline{V}_\gamma^{(k-1)}(s') + \gamma \underline{\delta}_k \right\} \\ &\geq \min \left\{ \underline{l}(s), \max_{u \in \mathcal{U}} \min_{s' \in \Delta(s, u)} \gamma \underline{V}_\gamma^{(k-1)}(s') \right\} + \gamma \underline{\delta}_k \\ &= \underline{V}_\gamma^{(k)}(s) + \gamma \underline{\delta}_k, \end{aligned}$$

where the second inequality follows from the fact that $\min\{a, b + c\} \geq \min\{a, b\} + c$, for any $c \leq 0$. \square

Applying Lemma 1 recursively allows us to bound the distance from the fixed point.

Corollary 1. Fix any iteration $k \in \mathbb{N}$ of the value iteration algorithm computing \underline{V}_γ . Then, $\forall s \in S$,

$$\underline{V}_\gamma(s) \geq \underline{V}_\gamma^{(k)}(s) + \frac{\gamma \underline{\delta}_k}{1 - \gamma}.$$

PROOF. By Lemma 1, we have

$$\forall s \in S, \underline{V}_\gamma^{(k+1)}(s) \geq \underline{V}_\gamma^{(k)}(s) + \gamma \underline{\delta}_k.$$

Thus, $\underline{\delta}_{k+1} \leq \gamma \underline{\delta}_k$. Applying the lemma inductively results in

$$\underline{V}_\gamma^{(k+2)}(s) \geq \underline{V}_\gamma^{(k+1)}(s) + \gamma^2 \underline{\delta}_k \geq \underline{V}_\gamma^{(k)}(s) + \gamma \underline{\delta}_k + \gamma^2 \underline{\delta}_k.$$

Thus, $\forall h \in \mathbb{N}$,

$$\underline{V}_\gamma^{(k+h)}(s) \geq \underline{V}_\gamma^{(k)}(s) + \underline{\delta}_k \sum_{i=1}^h \gamma^i.$$

Therefore,

$$\underline{V}_\gamma(s) = \lim_{h \rightarrow \infty} \underline{V}_\gamma^{(k+h)}(s) \geq \underline{V}_\gamma^{(k)}(s) + \underline{\delta}_k \sum_{i=1}^{\infty} \gamma^i = \underline{V}_\gamma^{(k)}(s) + \frac{\gamma \underline{\delta}_k}{1 - \gamma}.$$

\square

We now analyze the consequences of early stopping on \bar{V}_γ .

Lemma 2. Fix any iteration $k \in \mathbb{N}$ of the value iteration algorithm computing \bar{V}_γ . Then, $\forall s \in S$,

$$\bar{V}_\gamma^{(k+1)}(s) \leq \bar{V}_\gamma^{(k)}(s).$$

PROOF. The proof follows similar steps to those of the proof of Lemma 1. We proceed by induction. Base case: by definition,

$$\bar{V}_\gamma^{(1)}(s) = \min \left\{ \bar{l}(s), \max_{u \in \mathcal{U}} \max_{s' \in \Delta(s, u)} \gamma \bar{V}_\gamma^{(0)}(s') \right\}.$$

Thus, $\forall s \in S, \bar{V}_\gamma^{(1)}(s) \leq \bar{l}(s)$, and the latter is equal to $\bar{V}_\gamma^{(0)}(s)$, proving the base case. Next, fix a $k \geq 0$ and assume now for the sake of induction that $\forall s \in S, \bar{V}_\gamma^{(k+1)}(s) \leq \bar{V}_\gamma^{(k)}(s)$. We will prove that $\forall s \in S, \bar{V}_\gamma^{(k+2)}(s) \leq \bar{V}_\gamma^{(k+1)}(s)$. Again, by definition, $\forall s \in S$,

$$\bar{V}_\gamma^{(k+2)}(s) = \min \left\{ \bar{l}(s), \max_{u \in \mathcal{U}} \max_{s' \in \Delta(s, u)} \gamma \bar{V}_\gamma^{(k+1)}(s') \right\}.$$

However, $\forall s' \in S, \bar{V}_Y^{(k+1)}(s') \leq \bar{V}_Y^{(k)}(s')$, by the induction hypothesis. Thus, $\forall s \in S$,

$$\bar{V}_Y^{(k+2)}(s) \leq \min \left\{ \bar{l}(s), \max_{u \in \mathcal{U}} \max_{s' \in \Delta(s, u)} \gamma \bar{V}_Y^{(k)}(s') \right\}.$$

But the right-hand-side of the inequality above is equal to $\bar{V}_Y^{(k+1)}(s)$, by definition. Consequently, $\forall s \in S, \bar{V}_Y^{(k+2)}(s) \leq \bar{V}_Y^{(k+1)}(s)$. \square

Corollary 2. For any iteration $k \in \mathbb{N}$ of the value iteration algorithm computing \bar{V}_Y with initialization $\bar{V}_Y^{(0)}(s) = \bar{l}(s)$ for all $s \in S$, we have that $\forall s \in S$,

$$\bar{V}_Y(s) \leq \bar{V}_Y^{(k)}(s).$$

PROOF. By Lemma 2, the sequence $\{\bar{V}_Y^{(k)}\}_{k \in \mathbb{N}}$ is monotonically entry-wise decreasing and \bar{V}_Y is its fixed point, by definition. \square

Both Corollaries 1 and 2 hold if \bar{V}_Y was replaced by \bar{V}_Y^A and \underline{V}_Y was replaced by \underline{V}_Y^A , respectively.

7 Algorithm description and guarantees

Corollaries 1 and 2 allow constructing conservative value function bounds. Algorithm 1 implements value iteration with early stopping based on two user-specified parameters: $\underline{\delta}^* \leq 0$ for the lower bound and $\bar{\delta}^* > 0$ for the upper bound.

For the lower bound, the algorithm iterates until

$$\underline{\delta}_k := \min_{s \in S} (V_Y^{A, (k)}(s) - V_Y^{A, (k-1)}(s)) \geq \underline{\delta}^*.$$

For the upper bound, the algorithm iterates until

$$\|\bar{V}_Y^{A, (k)} - \bar{V}_Y^{A, (k-1)}\| < \bar{\delta}^*.$$

Upon satisfying both stopping conditions, the algorithm applies the correction term derived in Corollary 1 to obtain the conservative lower bound $\underline{V}_Y^{\text{cons}}$, while using $\bar{V}_Y^{(k)}$ directly as \bar{V}_Y^{cons} . Smaller values of $|\underline{\delta}^*|$ and $|\bar{\delta}^*|$ result in tighter lower and upper bounds at the cost of more value iteration steps. Theorem 2 establishes that these bounds provide sound classification of safe and unsafe cells in \mathcal{G} .

Theorem 2. Let $\underline{V}_Y^{\text{cons}}, \bar{V}_Y^{\text{cons}} : S \rightarrow \mathbb{R}$ be the value functions produced by Algorithm 1. Then, for any $s \in S$,

$$\underline{V}_Y^{\text{cons}}(s) > 0 \implies [[s]] \cap \mathcal{L} = \emptyset. \quad (10)$$

Moreover, if \mathcal{U} is finite and $A = \mathcal{U}$, then

$$\bar{V}_Y^{\text{cons}}(s) \leq 0 \implies [[s]] \subseteq \mathcal{L}. \quad (11)$$

PROOF. First, recall from Section 5 that $\forall s \in S, \forall x \in [[s]], V_Y(s) \leq V_Y(x) \leq \bar{V}_Y(s)$.

Then, using Corollaries 1 and 2, and noting that if $A \subseteq \mathcal{U}$, then $\max_{u \in \mathcal{U}}$ in (8) will be taken over a subset of \mathcal{U} in Algorithm 1, and this results in $\underline{V}_Y^A(s) \leq \underline{V}_Y(s) \forall s \in S$, and if $A = \mathcal{U}$, then $\underline{V}_Y^A(s) = \underline{V}_Y(s) \forall s \in S$, then we obtain the following inequality: for any $s \in S$ and $x \in [[s]]$,

$$\underline{V}_Y^{\text{cons}}(s) \leq \underline{V}_Y^A(s) \leq \underline{V}_Y(s) \leq V_Y(s) \leq \bar{V}_Y(s). \quad (12)$$

Algorithm 1 Computing sound bounds on V_Y

```

1: Input: continuous state space  $X \in \mathbb{R}^n$ , action space  $U$ , vector field  $f$ , failure function bounds  $\underline{l}$  and  $\bar{l}$ , discount factor  $\gamma > 0$ , initial uniform grid resolution  $\epsilon > 0$ , Lipschitz constants  $L_f$  and  $L_l$ , stopping condition parameters,  $\underline{\delta}^* \leq 0$  and  $\bar{\delta}^* > 0$ 
2: Create a grid  $\mathcal{G}$  with uniform resolution  $\epsilon$  over  $X$ 
3: for  $s \in S$  do
4:   Initialize:  $\underline{V}_Y^{A, (0)}(s) \leftarrow \underline{l}(s), \bar{V}_Y^{A, (0)}(s) \leftarrow \bar{l}(s)$ 
5: end for
6:  $k \leftarrow 0$ 
7: while  $\underline{\delta}_k := \min_{s \in S} (\underline{V}_Y^{A, (k)}(s) - \underline{V}_Y^{A, (k-1)}(s)) < \underline{\delta}^* \quad \text{or}$ 
    $\|\bar{V}_Y^{A, (k)} - \bar{V}_Y^{A, (k-1)}\| \geq \bar{\delta}^*$  do
8:   for  $s \in S$  do
9:     Initialize:  $\underline{v} \leftarrow -\infty, \bar{v} \leftarrow -\infty$ 
10:    for  $a \in A$  do
11:      Compute  $\Delta(s, a)$ 
12:       $\underline{v} \leftarrow \max\{\underline{v}, \min_{s' \in \Delta(s, a)} \gamma \underline{V}_Y^{A, (k)}(s')\}$ 
13:       $\bar{v} \leftarrow \max\{\bar{v}, \max_{s' \in \Delta(s, a)} \gamma \bar{V}_Y^{A, (k)}(s')\}$ 
14:    end for
15:     $\underline{V}_Y^{A, (k+1)}(s) \leftarrow \min\{\underline{l}(s), \underline{v}\}$ 
16:     $\bar{V}_Y^{A, (k+1)}(s) \leftarrow \min\{\bar{l}(s), \bar{v}\}$ 
17:  end for
18:   $k \leftarrow k + 1$ 
19: end while
20: for  $s \in S$  do
21:    $\underline{V}_Y^{\text{cons}}(s) \leftarrow \underline{V}_Y^{A, (k)}(s) + \frac{\gamma \delta_k}{1-\gamma}$ 
22:    $\bar{V}_Y^{\text{cons}}(s) \leftarrow \bar{V}_Y^{A, (k)}(s)$ 
23: end for
24: return  $\underline{V}_Y^{\text{cons}}, \bar{V}_Y^{\text{cons}}$ 

```

Suppose $\underline{V}_Y^{\text{cons}}(s) > 0$, by the inequality above we have $\forall x \in [[s]], V_Y(x) > 0$. By the definition of the unsafe set \mathcal{L} , a state x belongs to \mathcal{L} if and only if $V_Y(x) \leq 0$. Since $V_Y(x) > 0 \forall x \in [[s]]$, we conclude that no state in $[[s]]$ belongs to \mathcal{L} , i.e., $[[s]] \cap \mathcal{L} = \emptyset$, proving (10).

Now suppose that \mathcal{U} is finite, $A = \mathcal{U}$, and $\bar{V}_Y^{\text{cons}}(s) \leq 0$. Then, $\bar{V}_Y^A = \bar{V}_Y$. Moreover, by Corollary 2, we have that for any $s \in S$ and $x \in [[s]], V_Y(x) \leq \bar{V}_Y(s) \leq \bar{V}_Y^{\text{cons}}(s)$. Thus, for any $s \in S$ and $x \in [[s]]$, we have $V_Y(x) \leq 0$. By the definition of \mathcal{L} , this means that every state $x \in [[s]]$ satisfies $x \in \mathcal{L}$. Therefore, $[[s]] \subseteq \mathcal{L}$, proving (11). \square

Theorem 2 allows determining a set of safe states in the general case when $A \subseteq \mathcal{U}$ and determining a set of unsafe states when \mathcal{U} is finite and $A = \mathcal{U}$. However, for cells where $\underline{V}_Y^{\text{cons}}(s) \leq 0 < \bar{V}_Y^{\text{cons}}(s)$ or where $\underline{V}_Y^{\text{cons}}(s) \leq 0$ and $A \subset \mathcal{U}$, the theorem does not determine whether the cell is safe or unsafe. Such cells may contain both safe and unsafe continuous states. One can conservatively consider them as unsafe to over-approximate \mathcal{L} . However, the classification of these cells depends on their sizes. A coarse grid may result in many unclassified cells and consequently to a coarse over-approximation of \mathcal{L} . To achieve more accurate over-approximation of \mathcal{L} , one can

refine the unclassified cells by dividing them into smaller ones and recomputing the value function bounds until the desired accuracy is achieved.

8 Refining unclassified cells

We now present a refinement algorithm that splits the unclassified cells to more accurately over-approximate \mathcal{L} . Upon termination of Algorithm 1, the cells in grid \mathcal{G} are classified into three disjoint classes:

- **Safe cells:** $\{s \in S \mid \underline{V}_\gamma^{\text{cons}}(s) > 0\}$,
- **Unsafe cells:** $\{s \in S \mid \mathcal{U} \text{ is finite, } A = \mathcal{U}, \overline{V}_\gamma^{\text{cons}}(s) \leq 0\}$,
- **Unclassified cells:** any cell not in the previous two sets.

Algorithm 2 implements a refinement scheme that splits unclassified cells. Each unclassified cell s is split along its longest side into two equally-sized cells. Failure function and value function bounds are recomputed via Algorithm 1 on the refined grid. This process is repeated until all unclassified cells have been refined to a user-defined minimum resolution.

Algorithm 2 Adaptive refinement of boundary cells

```

1: Input:  $\mathcal{G}, \epsilon_{\min}$ 
2: Run Algorithm 1 on  $\mathcal{G}$  to initialize  $\underline{V}_\gamma^{\text{cons}}, \overline{V}_\gamma^{\text{cons}}$ 
3:  $\text{queue} \leftarrow \{s \in S \mid \overline{V}_\gamma^{\text{cons}}(s) > 0 \wedge \underline{V}_\gamma^{\text{cons}}(s) \leq 0\}$ 
4: while  $\text{queue} \neq \emptyset$  do
5:   Dequeue a cell  $s$  from  $\text{queue}$ 
6:   Let  $j^* = \arg \max_j \eta_j(s)$ 
7:   if  $\eta_{j^*}(s) > \epsilon_{\min}$  then
8:     Split  $s$  into two cells  $s_1$  and  $s_2$  along the  $j^*$ th axis
9:     Recompute  $\overline{V}_\gamma^{\text{cons}}$  and  $\underline{V}_\gamma^{\text{cons}}$  over the new grid
10:    if  $\overline{V}_\gamma^{\text{cons}}(s_1) > 0 \wedge \underline{V}_\gamma^{\text{cons}}(s_1) \leq 0$  then
11:      Enqueue  $s_1$  in  $\text{queue}$ 
12:    end if
13:    if  $\overline{V}_\gamma^{\text{cons}}(s_2) > 0 \wedge \underline{V}_\gamma^{\text{cons}}(s_2) \leq 0$  then
14:      Enqueue  $s_2$  in  $\text{queue}$ 
15:    end if
16:  end if
17: end while
18: return  $\underline{V}_\gamma^{\text{cons}}, \overline{V}_\gamma^{\text{cons}}$ 

```

Remark 1. After the termination of Algorithm 2, all remaining unclassified cells, if any, can be conservatively labeled as unsafe, resulting in an over-approximation of the unsafe set \mathcal{L} .

Theorem 3. Algorithms 1 and 2 terminate in finite time.

PROOF. We first establish that Algorithm 1 terminates in finite time. The while loop condition at line 3 of Algorithm 1 checks whether

$$\delta_k := \min_{s \in S} \left(\overline{V}_\gamma^{A,(k)}(s) - \underline{V}_\gamma^{A,(k-1)}(s) \right) < \underline{\delta}^*, \quad (13)$$

$$\left\| \overline{V}_\gamma^{A,(k)} - \overline{V}_\gamma^{A,(k-1)} \right\| \geq \overline{\delta}^*. \quad (14)$$

By Theorem 1, the Bellman operators are γ -contractions, so the value iteration sequences converge to their respective fixed points.

This ensures that $\underline{\delta}_k \rightarrow 0$ and $\left\| \overline{V}_\gamma^{A,(k)} - \overline{V}_\gamma^{A,(k-1)} \right\| \rightarrow 0$ as $k \rightarrow \infty$, guaranteeing that the stopping conditions are eventually satisfied in a finite number of iterations. Therefore, Algorithm 1 terminates in finite time.

Now we prove that Algorithm 2 terminates. The initial grid \mathcal{G} has a uniform resolution of ϵ . Each iteration of the while loop removes one cell s from the queue and potentially splits it into two cells s_1, s_2 by splitting along the dimension j^* with the longest side. A cell can be split at most $(\frac{\epsilon}{\epsilon_{\min}})^n$ times before reaching $\eta_{j^*}(s) \leq \epsilon_{\min}$ in all dimensions, at which point it is no longer refined (line 8). Since the initial grid has a finite size and each cell can undergo only finitely many splits, the total number of refinement operations is bounded. Moreover, each call to Algorithm 1 at line 9 terminates in finite time. Therefore, Algorithm 2 terminates in finite time. \square

9 Case studies

In this section, we evaluate our method using two case studies: (1) Dubins car and (2) 3D evasion. We first introduce both tasks and then we showcase the results of applying our method (Algorithm 2) and existing methods [9] on these tasks.

9.1 Tasks

First, we describe the setup of each of the two tasks.

9.1.1 Dubins car. We consider a Dubins car model with dynamics:

$$\dot{x} = \frac{d}{dt} \begin{bmatrix} x_1 \\ x_2 \\ x_3 \end{bmatrix} = \begin{bmatrix} v \cos x_3 \\ v \sin x_3 \\ u \end{bmatrix},$$

where $[x_1, x_2]^\top \in \mathbb{R}^2$ represents the position of the vehicle in the plane, and $x_3 \in [-\pi, \pi]$ denotes its heading angle. The vehicle moves with constant velocity $v > 0$, and the control input $u \in [-1, 1]$ specifies the angular velocity.

The failure function is defined as the signed distance to a cylindrical obstacle centered at $[x_{\text{obs}}, y_{\text{obs}}]^\top$ with radius r :

$$l(x) = \sqrt{(x_1 - x_{\text{obs}})^2 + (x_2 - y_{\text{obs}})^2} - r.$$

9.1.2 3D evasion. We consider a three-dimensional aircraft evasion scenario used in [12] with dynamics:

$$\dot{x} = \frac{d}{dt} \begin{bmatrix} x_1 \\ x_2 \\ x_3 \end{bmatrix} = \begin{bmatrix} -v + v \cos x_3 + ux_2 \\ v \sin x_3 - ux_1 \\ -u \end{bmatrix},$$

where $[x_1, x_2]^\top \in \mathbb{R}^2$ denotes the relative planar position between the pursuer and evader, and $x_3 \in [-\pi, \pi]$ represents the relative heading angle. The pursuer moves with constant velocity $v > 0$, while the evader controls its angular velocity $u \in [-1, 1]$. The failure function is defined as the signed distance to a cylindrical collision region of unit radius:

$$l(x) = \sqrt{x_1^2 + x_2^2} - 1.$$

9.2 Results

Now, we compare the outputs of our method (Algorithm 2) and existing methods [9] and we briefly discuss some computational aspects of our method. In our implementation of Algorithm 2, rather

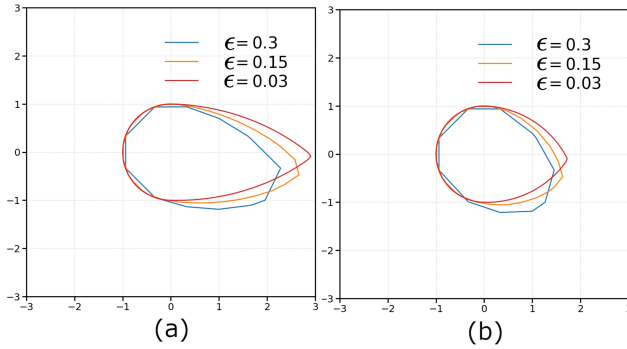


Figure 1: Contour plots of the unsafe set boundary computed using the existing HJ reachability toolbox [9] with different grid resolutions for (a) the 3D evasion ($v=1$) and (b) the Dubins car ($v=1$). In both cases, it is evident how lower grid resolutions underestimate the unsafe set, i.e., the backward reachable set.

than splitting cells individually, we dequeue and split all unclassified cells simultaneously in each iteration, then recompute \bar{V}_y^{cons} and $\underline{V}_y^{\text{cons}}$ over the refined grid. This approach is more computationally efficient than dequeuing one cell at a time and re-running value iteration for the whole grid. We refer to this batch refinement and value function recomputation as one iteration (itr) when running Algorithm 2 in Figures 2, 3, 4 and 5.

We construct discrete-time dynamics from the continuous-time ones using a set of sampling times $\{\tau_j\}_j$. For any τ_j , the discrete-time transition is defined as $x_{k+1} = \xi(x_k, a_j, \tau_j)$, which is computed by numerically integrating the continuous-time dynamics starting from x_k over the time interval $[0, \tau_j]$ with the constant control signal a_j that is equal to a and of duration τ_j . For the Dubins car, we use 3 discrete actions $A = \{-1, 0, 1\}$ and $\{\tau_j\}_j = \{0.25, 0.5\}$, while for the 3D evasion task, we use 5 discrete actions $A = \{-1, -0.5, 0, 0.5, 1\}$ and $\{\tau_j\}_j = \{0.2, 0.4, 0.6\}$.

9.2.1 Comparison of our method to existing methods. Figure 1 shows how existing methods ([9, 13]) for computing the HJ reachability value function result in under-approximations of the unsafe set \mathcal{L} when using low grid resolutions (i.e., large ϵ). Specifically, one can see that there are states that are considered as part of the approximation of \mathcal{L} when using an $\epsilon = 0.03$ but are not part of it when using an $\epsilon = 0.3$ while the former should be more accurate than the latter. That indicates that there are potentially states that are unsafe that are mislabeled as safe when using $\epsilon = 0.3$.

On the other hand, Figures 2 and 3 show the outputs of Algorithm 2 at different iterations, we can see that our method does not mislabel unsafe cells as safe at any grid resolution, as mentioned in Theorem 2. We can also see how as we run more refinement iterations (itr), further refining unclassified cells, the algorithm is able to more accurately classify the safe and unsafe sets. Zooming into itr. 23 in Figure 2 and itr. 21 in Figure 3 shows how cells at the boundary are much finer than the regions of the state space that are more easily classifiable as safe or unsafe.

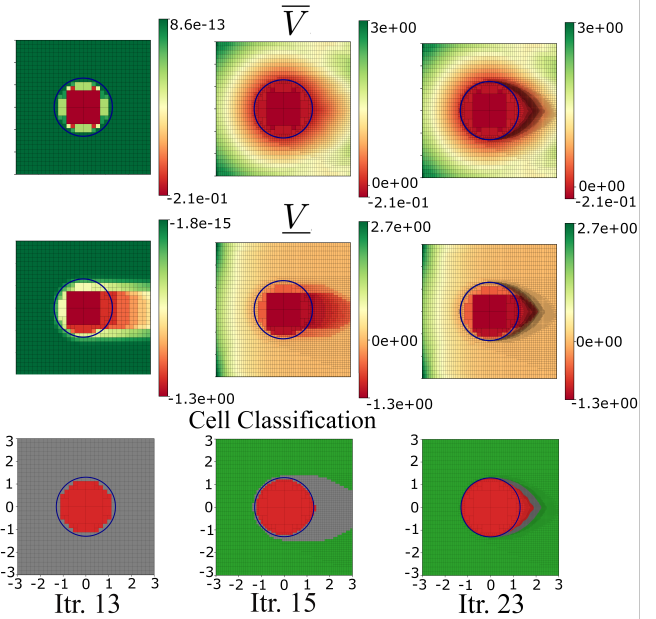


Figure 2: Output of Algorithm 2 at different iterations (itr) for the Dubins car with $\gamma = 0.9$, $v = 1$, $\underline{\delta}^* = 10^{-13}$, $\bar{\delta}^* = 10^{-13}$ and $\theta = \pi$. Cells are classified as: green when $\underline{V}^{\text{cons}} > 0$, red when $\bar{V}^{\text{cons}} < 0$.

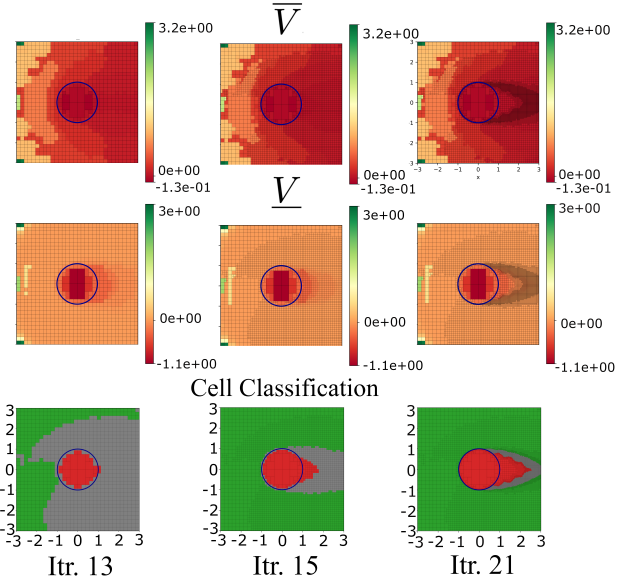


Figure 3: Output of Algorithm 2 at different iterations (itr) for the 3D evasion task with $\gamma = 0.3$, $v = 1$, $\underline{\delta}^* = 10^{-13}$, $\bar{\delta}^* = 10^{-15}$ and $\theta = \pi$. Cells are classified as: green when $\underline{V}^{\text{cons}} > 0$, red when $\bar{V}^{\text{cons}} < 0$.

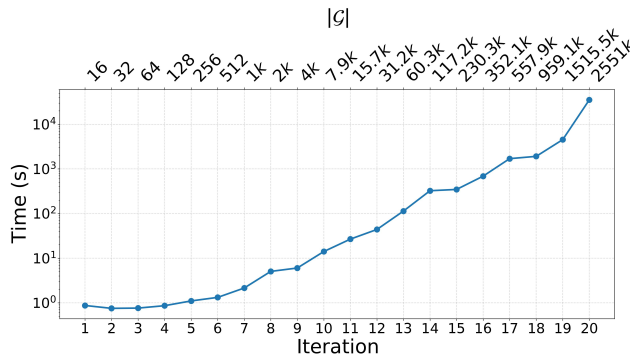


Figure 4: Computational performance of Algorithm 2 on the 3D evasion task. Time per iteration includes boundary cell refinements, successor set computation, value iteration over the entire grid, and visualization. The x-axis shows iteration numbers and corresponding grid sizes $|\mathcal{G}|$. All experiments were conducted on an Apple MacBook M3 Pro laptop.

9.2.2 Computational time. Figures 4 and 5 illustrate the computational performance of Algorithm 2 on the 3D evasion and Dubins tasks, tracking runtime per iteration as the grid is refined. All experiments were conducted on an Apple MacBook M3 Pro laptop. Runtime includes unclassified cells’ refinements, successor set computation, value iteration over the entire grid, and visualization such as generating Figures 2 and 3. The results show that the iteration time grows almost linearly with the grid size $|\mathcal{G}|$, which in turn grows exponentially every iteration. This growth in computational cost reflects the increased complexity of value iteration and successor set computation over progressively finer grids. We note that in Figure 2, there is a decrease in computation time after phase 14, even though $|\mathcal{G}|$ increases, and this is because iterations 15 till 21 require 14-77 steps of value iteration to reach the stopping condition in Algorithm 1 line 7 instead of 270+ steps that are required in iterations 1 till 14.

10 Conclusion

We presented an approach that computes sound and accurate over-approximations of the backward reachable sets of nonlinear discrete-time control systems using HJ reachability analysis. Our method performs value iteration over finite grids over the state space to construct provable upper and lower bounds on the discounted HJ reachability value function. It accounts for discretization errors in the state and action spaces and early termination of the value iteration algorithm. The obtained bounds are used to classify the cells in the grid over the state space as safe or unsafe. We also introduced a refinement algorithm that splits hard-to-classify cells to more accurately capture the unsafe set. We demonstrate its effectiveness in two case studies.

11 Limitations & future work

While our framework provides formal soundness guarantees for HJ reachability analysis, several directions remain for future investigation. The computational bottleneck of our approach lies in

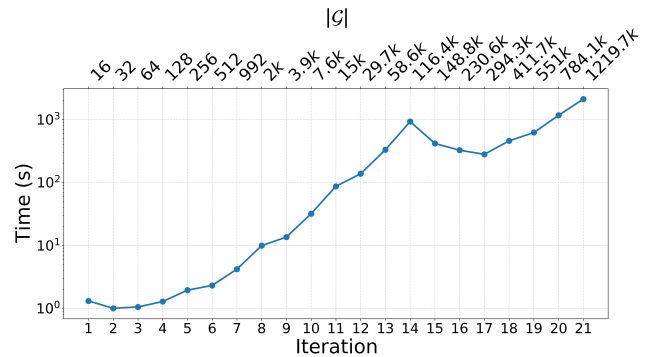


Figure 5: Computational performance of Algorithm 2 on the Dubins task. Time per iteration includes boundary cell refinements, successor set computation, value iteration over the entire grid, and visualization. The x-axis shows iteration numbers and corresponding grid sizes $|\mathcal{G}|$. All experiments were conducted on an Apple MacBook M3 Pro laptop.

computing successor sets and performing value iteration over the entire grid at each refinement step, which could be significantly accelerated through GPU parallelization and more efficient local update schemes that propagate changes only through cells affected by refinement rather than performing global value iteration [16].

Moreover, there are several sources of over-approximation errors in our method including the over-approximation errors when computing the transition relation Δ because of the over-approximation errors when computing the forward reachable sets and discretizing the control space. One can address the former by using more accurate forward reachability analysis tools that utilize local continuity properties [6]. Also, one can address the latter by designing a refinement algorithm that refines the grid over the control space, not just the state space, to obtain more accurate over-approximation of the unsafe set.

Future work should also investigate deriving bounds on $|\bar{V}_\gamma^{\text{cons}}(s) - V_\gamma^{\text{cons}}(s)|$ as a function of η . This would enable the computation of a minimum grid resolution ϵ_{\min} over the state space that when used, one can guarantee that the computed bounds approximate the true value function, and thus the BRS as well, to a user-specified accuracy.

Finally, an essential extension of this work is addressing the same problem for continuous-time systems.

References

- [1] S. B. Alaoui and A. Saoud. How to discretize continuous state-action spaces in q-learning: A symbolic control approach. In *2024 IEEE 63rd Conference on Decision and Control (CDC)*, pages 8314–8319. IEEE, 2024.
- [2] A. D. Ames, S. Coogan, M. Egerstedt, G. Notomista, K. Sreenath, and P. Tabuada. Control barrier functions: Theory and applications. In *2019 18th European control conference (ECC)*, pages 3420–3431. Ieee, 2019.
- [3] A. D. Ames, X. Xu, J. W. Grizzle, and P. Tabuada. Control barrier function based quadratic programs for safety critical systems. *IEEE Transactions on Automatic Control*, 62(8):3861–3876, 2017.
- [4] M. Bui, G. Giovanis, M. Chen, and A. Shriram. Optimizedddp: An efficient, user-friendly library for optimal control and dynamic programming. *arXiv preprint arXiv:2204.05520*, 2022.
- [5] L. Chen, P. Wu, K. Chitta, B. Jaeger, A. Geiger, and H. Li. End-to-end autonomous driving: Challenges and frontiers. *IEEE Transactions on Pattern Analysis and Machine Intelligence*, 2024.

[6] C. Fan, J. Kapinski, X. Jin, and S. Mitra. Locally optimal reach set over-approximation for nonlinear systems. In *Proceedings of the 13th International Conference on Embedded Software, EMSOFT '16*, New York, NY, USA, 2016. Association for Computing Machinery.

[7] T. Haidegger. Autonomy for surgical robots: Concepts and paradigms. *IEEE Transactions on Medical Robotics and Bionics*, 1(2):65–76, 2019.

[8] K. L. Hobbs, M. L. Mote, M. C. Abate, S. D. Coogan, and E. M. Feron. Runtime assurance for safety-critical systems: An introduction to safety filtering approaches for complex control systems. *IEEE Control Systems Magazine*, 43(2):28–65, 2023.

[9] S. A. S. Lab. `hj_reachability`: Hamilton–jacobi reachability analysis in jax. https://github.com/StanfordASL/hj_reachability, 2024. GitHub repository.

[10] S. A. S. Lab. `hj_reachability`: Hamilton–jacobi reachability analysis in jax. https://github.com/StanfordASL/hj_reachability, 2024. GitHub repository.

[11] J. Li, D. Lee, J. Lee, K. S. Dong, S. Sojoudi, and C. Tomlin. Certifiable reachability learning using a new lipschitz continuous value function. *IEEE Robotics and Automation Letters*, 2025.

[12] J. Liu and E. Mallada. Recurrent control barrier functions: A path towards nonparametric safety verification, 2025.

[13] I. M. Mitchell, A. M. Bayen, and C. J. Tomlin. A time-dependent hamilton–jacobi formulation of reachable sets for continuous dynamic games. *IEEE Transactions on automatic control*, 50(7):947–957, 2005.

[14] I. M. Mitchell and J. A. Templeton. A toolbox of hamilton–jacobi solvers for analysis of nondeterministic continuous and hybrid systems. In *International workshop on hybrid systems: computation and control*, pages 480–494. Springer, 2005.

[15] P. Tabuada. *Verification and control of hybrid systems: a symbolic approach*. Springer Science & Business Media, 2009.

[16] S. Tonkens, A. Toofanian, Z. Qin, S. Gao, and S. Herbert. Patching approximately safe value functions leveraging local hamilton–jacobi reachability analysis. In *2024 IEEE 63rd Conference on Decision and Control (CDC)*, pages 3577–3584. IEEE, 2024.